104 (2025) 104595

Contents lists available at ScienceDirect

Poultry Science

journal homepage: www.elsevier.com/locate/psj

Full-Length Article

Dielectric spectroscopy and TD-NMR investigation for assessing water solid dynamics in normal and wooden breast chicken

Francesca Soglia [a,b], Eleonora Iaccheri [a,b], Luca Laghi [a,b], Luigi Ragni [a,b], Pedro José Fito Suñer [c], Massimiliano Petracci [a,b,*]

[a] Interdepartmental Centre for Agri-Food Industrial Research, Alma Mater Studiorum, University of Bologna, Cesena, Italy
[b] Department of Agricultural and Food Sciences, Alma Mater Studiorum, University of Bologna, Cesena, Italy
[c] Institute of Food Technology Food UPV, Universitat Politecnica de Valencia, Valencia, Spain

ARTICLE INFO

Keywords:
NMR
Dielectric spectroscopy
Wooden breast chicken
Water mobility
Relaxation

ABSTRACT

Dielectric Spectroscopy (DS) and TimeDomain-Nuclear Magnetic Resonance (TD-NMR) were exploited to investigate water and solid dynamics in chicken's *Pectoralis major* muscles having macroscopically normal appearance (N) and affected by Wooden Breasts (WB) abnormality. 147 PMM were collected and classified as macroscopically normal (N) (N=74) or Wooden Breast (WB) (N=73) based on their visual appearance and manual palpation. Protons' T_2 (transverse relaxation time), and dielectric properties were carried out. The dielectric constant ($\varepsilon' = 62.0$) and the loss factor ($\varepsilon'' = 19.7$) of γ relaxation of WB samples was significantly higher than the one of N samples ($\varepsilon' = 59.8$ and $\varepsilon'' = 18.3$), while the WB revealed a low relaxation frequency (1.5 E+09) compared to N samples (1.7 E+09). WB showed a higher dielectric constant of relaxation and thus polarizability mainly due to free water, and lower relaxation frequency imputable to a more complex solid structure. This was confirmed by TD-NMR, evidencing a significant increase in the relative intensity of the proton population ascribable to the extra-myofibrillar water (32.9 *vs.* 21.5%; P<0.001) along with a reduction of the one occupying the intra-myofibrillar spaces (62.0 *vs.* 75.4%; P<0.001). These outcomes may be ascribed to the re-organization of the skeletal muscle structure associated with the onset and progression of the WB abnormality.

Introduction

Over the past half-century, the selection practices have improved broilers' growth performance and meat yield (Barbut et al., 2024). These, however, have led to an increased susceptibility of the birds to stressors and, concurrently, resulted in an increased incidence of growth-related abnormalities affecting the *Pectoralis major* muscles (PMM) (Barbut et al., 2024; Soglia et al., 2021). Among them, the Wooden Breast (WB) defect worsens the main quality traits and technological properties of breast meat, including its water-holding capacity (WHC), mechanical properties, and nutritional profile (Pang et al., 2020; Wang et al., 2023). These modifications mirror a substantial re-organization of the muscular architecture, which can be observed at the microscopic level. Indeed, WB-affected muscles usually exhibit histological features that profoundly differ from those of the unaffected cases (Normal - N), including fiber necrosis along with occasional regeneration processes and proliferation of connective tissue (fibrosis) both at peri- and endo-mysial level (Soglia et al., 2021). In addition, the inflammatory processes associated with WB, as well as the reduced protein content in the affected PMM, ultimately result in an impaired water-holding ability (Dalgaard et al., 2018; Soglia et al., 2021). Studying the dynamics of biological macromolecules, such as water-protein interaction, is of utmost importance for understanding the physical state changes affecting the protein structures and, thus, their related biological function (Schmidt, 2004). Dielectric spectroscopy (DS) and time-domain nuclear magnetic resonance (TD-NMR) are two leading methods to describe protein-water dynamics. DS and TD-NMR are based on different physical principles, but both look at the biological matrix's movements related to dipole moments.

Dielectric spectroscopy studies a material's permittivity, the response to applying an electromagnetic field. When a biological material is subjected to an electromagnetic field, different phenomena simultaneously occur. Part of the wave energy is stored by the material's components' polarization, considered by the parameter called dielectric

* Corresponding author at: Department of Agricultural and Food Sciences, Alma Mater Studiorum, University of Bologna, P.zza Goidanich, 60, Cesena, FC, Italy.
E-mail address: m.petracci@unibo.it (M. Petracci).

https://doi.org/10.1016/j.psj.2024.104595
Received 10 September 2024; Accepted 25 November 2024
Available online 26 November 2024

constant. Another phenomenon is the frictional motion of the sample constituents leading to heat, the so-called loss factor (Debye, 1934; Markx and Davey, 1999). Space charge accumulation on the material's surface, electric dipole orientation, and macrostructural polarization are some of the physical mechanisms proposed to explain the induced polarization (Lawrence et al., 1957). The study of these mechanisms can give information about the structures and composition of biological materials at the cellular and even molecular levels (Lawrence et al., 1957; Schwan and Foster, 1977). Dipolar polarization is mainly caused by the separation of a pair of opposite charges in either permanent dipoles, like water, or induced dipoles, such as those of non-polar molecules (Batyuk and Kizilova, 2018). The tendency of permittivity to decrease in steps as a function of frequency increases, giving rise to a dispersive behavior, reflects the loss of polarization induced by relaxation events (Debye, 1934; Kuang and Nelson, 1998; Lawrence et al., 1957). The relaxation events have characteristic times and frequencies, affecting the permittivity and causing dispersions (Debye, 1934; Kuang and Nelson, 1998; Markx and Davey, 1999). Biological materials show characteristics of dispersions, such as α, β, δ, and γ (Schwan and Foster, 1977). α-dispersion is revealed in the low-frequency range (10 Hz-10 KHz) and is mainly related to ionic content and mobility along the surfaces of the cells (Batyuk and Kizilova, 2018). For this reason, it is mainly recognized as conductivity. Accordingly, when the cell structure is considered, the α-dispersion allows to study the mechanisms occurring across the cell's membrane (Batyuk and Kizilova, 2018). The β-dispersion occurs at higher frequencies (10KHz-10 MHz) and is linked to the capacitive charging of the cellular membranes, a mechanism known as interfacial or Maxwell-Wagner polarization (Schwan and Foster, 1977). The β-dispersion is more influenced by water content than the α-dispersion. Less water in a biological tissue reduces the strength of the β-dispersion because the passage of ions is reduced by air gaps or dry elements (Kuang and Nelson, 1998). The γ -dispersion occurs in the microwave range, above a couple of hundred MHz. It is mainly attributed to the rotation of dipoles such as those represented by free water, small molecules like the intracellular electrolytes (Schwan and Foster, 1977), and polar proteins immersed in the aqueous medium (Wolf et al., 2012). The δ -dispersion generally occurs in the 0.1 – 5.0 GHz range, between β and γ dispersions' typical ranges, and is produced by the rotation of macromolecular side chains of large molecules, biopolymers, such as proteins and proteins bound to water, and cellular organelles (Batyuk and Kizilova, 2018). A relaxation frequency of bound water lower than the one of free water produces a weak dispersion that can be explained by several effects (Wolf et al., 2012). The electrical behavior of water in the proximity of other particles is different, depending on the kind of particle water interacts with (Batyuk and Kizilova, 2018). The α, β, δ and γ dispersions may therefore be described by total dielectric decrements $\Delta\varepsilon$ α, $\Delta\varepsilon$ β, $\Delta\varepsilon$ δ and $\Delta\varepsilon$ γ, respectively. The traditional approach to fit the electromagnetic spectrum to determine the different dispersions exploits the Debye or Cole-Cole equation (Cole and Cole, 1941; Debye, 1934). Debye's model is only applicable to purely polar compounds, so it is inappropriate for biological materials. The Cole-Cole equation and many other models previously proposed have been used to describe these relaxation mechanisms in natural materials, enabling the calculation of relaxation parameters (Asami, 2002; Gabriel et al., 1996; Havriliak and Negami, 1967; Hurt, 1985; Kuang and Nelson, 1998; Lawrence et al., 1957; Wolf et al., 2012). Still, there are concerns about these models, due to the complexity of their application. Accordingly, Traffano et al. developed, specifically for chicken meat, a modified Gompertz model (Traffano-Schiffo et al., 2017) able to define electromagnetic dispersions and to calculate the relaxation dielectric constant and frequencies of the different dispersions. According to such model, the distribution of the different relaxations can be related and used to investigate the material's physically involved processes (Batyuk and Kizilova, 2018).

NMR is a low-frequency electromagnetic technique (Hz, MHz region), associated with the spins of atoms' nuclei. The magnetic field exerts a torque force, inducing a spin nuclei-specific orientation with a defined energy level (Schmidt, 2004). Therefore, an NMR spectrum represents the energy required for energy level transitions to occur, allowing the observation of each active nucleus independently from the others, because characterized by a specific frequency of resonance (Schmidt, 2004). An observation by NMR starts when the oscillating magnetic field that induced the excitation of nuclei is interrupted, leading to the subsequent so-called relaxation. Relaxation is an energy loss process that can be observed both longitudinally or transversally to the magnetic field. The longitudinal relaxation time (T_1) is affected by local fluctuations between antiparallel and parallel spin positions. Many physical processes in food result from these local fluctuations induced by magnetic fields, such as the liquid dipole-dipole interactions (Kruk et al., 2020; O'Toole et al., 2023; Schmidt, 2004). The transverse relaxation time (T_2) is affected by the loss of phase of the spin and by the exchange of energy between identical nuclei. Both T_1 and T_2 relaxations have been related to water mobility. Accordingly, NMR T_1 and T_2 relaxation times can be used to investigate the dynamics of water and solids in food systems, despite their compositional and structural complexity.

Several authors have previously studied the dielectric properties of chicken meat in the radio-frequency range (Kent and Anderson, 1996; Nelson et al., 2007; Tanaka et al., 2000; Tran and Stuchly, 1987). Despite such interest, only a limited number of works are available on dielectric properties conducted on poultry muscle in connection with defects or abnormalities. An example is the work by Traffano-Schiffo et al., who measured the permittivity in the microwave range (500 MHz-20 GHz) of the whole chicken carcasses with skin, to study and detect white striping myopathy to develop a spectrophotometric-based sensor (Traffano-Schiffo et al., 2017). Another example is the work by Morey et al., who evaluated WB myopathy by using bioelectrical impedance to develop a rapid detection method (Morey et al., 2020).

NMR T_2 relaxation times have been used in the recent past to study the effect of WB abnormality on water holding capacity and rheological and gelling properties of chicken breast meat (Zhang et al., 2020).

Some authors have previously combined NMR relaxometry and Dielectric Spectroscopy to explore the interaction of water with single proteins, such as bovine elastin, lysozyme of hen egg white, and equine heart's myoglobin (Fukuzaki et al., 1995; Kruk et al., 2020). In these circumstances, the relaxation times computed by both techniques exhibited a poor correlation. Rather, the two techniques seemed to give complementary information about the slow, intermediate, and fast dynamics of whole proteins (Kruk et al., 2020). Few works can be traced combining NMR and DS techniques for the observation of complex systems, none of them focusing on WB myopathy.

Given this state of the art, DS relaxation parameters and TD-NMR properties will be shown in the present work for the first time, to enhance the understanding of water-protein dynamics in the breast of WB and N chickens. The outcomes from the two techniques will be compared by considering the different physical backgrounds of the two techniques. Theoretical dielectric characterization of the relaxation processes of the chicken breast could be exploited to develop a rapid sensor able to detect WB myopathy online.

Material and methods

Sample collection

A total of 147 PMM were collected 3 h *post-mortem* in the deboning area of a commercial slaughtering and processing plant. Breasts were selected from the same flock of fast-growing broilers (males, 42 days old, 2.8 kg average live weight) and classified based on their visual appearance and manual palpation as macroscopically normal (N) (N=74) or Wooden Breast (WB) (N=73) cases. To avoid misleading results only severe WB cases were considered and PMM showing any other defect (i.e., pale colour, white striations, detachment of the fiber bundles) were excluded.

Samples characterization

Meat quality analyses were performed to ascertain the effect of WB abnormality on Water Holding Capacity (WHC) and protein functionality. In detail, WHC was estimated by measuring the amount of fluid lost after i) 48h of refrigerated storage of a parallelepiped meat sample (8 × 4 × 2 cm, weighing about 70g) and ii) the subsequent application of heat treatment (under vacuum at 75°C in a water bath until reaching 72°C in the inner core of the heaviest sample by using the same subsample previously addressed to measure the amount of fluid lost during refrigerated storage).

Protein solubility was measured as an indirect index of their functionality, following the procedure described by Mudalal et al. (Mudalal et al., 2014) based on the method proposed by Warner et al. (Warner et al., 1997). Briefly, two aliquots of meat (weighing 1 g) were respectively homogenized (11,000 min^{-1} by means of a high-speed blender, Ultra-Turrax, T25 basic, New Brunswick, NJ) in 10 mL of 25 mM potassium phosphate buffer (pH 7.2) and 10 mL of 1.1 M KI, 0.1 M potassium phosphate (pH 7.2) buffer. After being stored for 20 h at 4°C, the homogenized samples were centrifuged (2,600 × g for 30 min at 4°C) and the protein concentration in the supernatant was measured by using the Bradford assay (Bradford, 1976) with bovine serum albumin as a standard.

The results obtained from the aforementioned analyses (WHC and protein solubility) have been analyzed by Student's t-test and considered significant at a p level < 0.05.

TD-NMR measurement

The T_2 proton relaxation times and intensities of all samples were measured by means of a Minispec MQ-20 spectrometer (Bruker Corporation, Karlsruhe, Germany) operating at 20 MHz. The Carr–Purcell–Meiboom–Gill (CPMG) pulse sequence was applied, with 180° pulses administered every 0.16 ms. Cylindrical samples with a diameter of 8 mm were obtained from both N and WB chicken breasts and placed in NMR tubes with an internal diameter of 10 mm (Petracci et al., 2012).

Dielectric properties measurement and fitting

Dielectric properties, such as dielectric constant (ε') and loss factor (ε''), were assessed by means of the instrumental chain shown in Fig. 1.

The measurements were conducted using an open-ended coaxial probe (DAKS-3.5 probe, Speag) and Vector Network Analyser (VNA), Copper Mountain R-140 interfaced via USB to a personal computer. A dedicated software (DAK Software Installer 2.6.1.7) acquires and transforms the reflected electrical signal in dielectric parameters. Calibration was performed with the DAK calibration kit (Speag DAK-3.5/1.2 Shorting Block, Metallic Strip Sets, and Tissue Simulating Liquid characterized by the value of dielectric permittivity of mid-range) accounting for open, short, and load assessment. The acquisitions were assessed in the frequency range from 200 MHz to 14 GHz. In the microwave range, cable movements must be avoided. Therefore, the coaxial probe was fixed with a stainless-steel support, and a moveable platform was used to keep samples in contact with the probe. Measurements were conducted in triplicate at 5(±1)°C. The real and imaginary components or complex relative permittivity can be expressed as:

$$\varepsilon^* = \varepsilon' - i\varepsilon'' \tag{1}$$

where real part ε' is the dielectric constant and imaginary part ε'' is the loss factor, and i is $\sqrt{-1}$.

Dielectric constant and loss factor were used to calculate relaxation parameters derived from the dispersion regions of the electromagnetic spectrum. The Gompertz modified equation is reported in Eq. (2).

$$l\varepsilon' = l\varepsilon'_{\infty} + \sum_{n=1}^{3} \frac{\Delta l'\varepsilon_n}{1 + e^{\left(l\omega^2 - l\omega_\tau^2\right)*\alpha_n}} \tag{2}$$

where $l\varepsilon'_{\infty}$ is the decimal logarithm of the dielectric constant at high frequencies, $\Delta l'\varepsilon_n$ is the magnitude of dispersion, $l\omega$ logarithm of the angular velocity (rad/s), $l\omega_\tau$ is the decimal logarithm of the angular velocity for each dispersion n, and α_n are the dispersion slopes. The angular velocity (rad/s) is calculated as 2π * f (frequency).

Afterward, the dielectric constant of *n*-relaxation (ε'_n) was calculated by Eqs. (3)–(5) (Traffano-Schiffo et al., 2017) by using Statgraphics software (Stagraphics 19-x64, Statgraphics Technologies, Inc).

$$\varepsilon'_{\alpha} = 10^{\left(l\varepsilon'_{\infty} + \Delta l\varepsilon'_{\gamma} + \Delta l\varepsilon'_{\beta} + \frac{\Delta l\varepsilon'_{\alpha}}{2}\right)} \tag{3}$$

$$\varepsilon'_{\beta} = 10^{\left(l\varepsilon'_{\infty} + \Delta l\varepsilon'_{\gamma} + \frac{\Delta l\varepsilon'_{\beta}}{2}\right)} \tag{4}$$

$$\varepsilon'_{\gamma} = 10^{\left(l\varepsilon'_{\infty} + \frac{\Delta l\varepsilon'_{\gamma}}{2}\right)} \tag{5}$$

The relaxation time (τ) was calculated as the reciprocal of the relaxation frequency (ω_c, rad/s).

Significant differences between the means of dielectric relaxation parameters for N and WB were evaluated by the Welsch's t-test (p-level < 0.05) for samples with non-homogeneous variance. The homogeneity of the variance was checked by means of Leven's test.

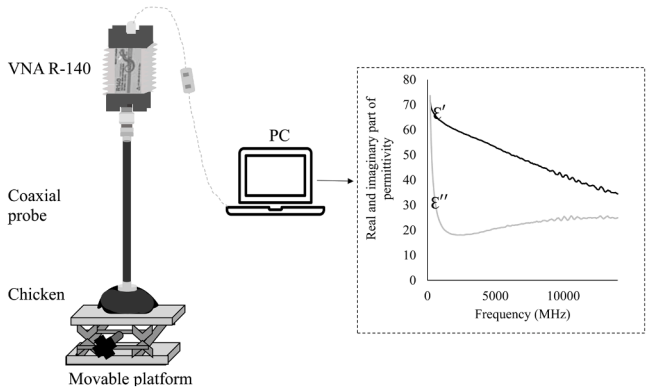

Fig. 1. Layout of the instrumental chain and spectral signal acquired.

Table 1
Means ± standard deviations of the parameters describing the Water Holding Capacity (drip and cooking loss) as well as the functionality of the protein fractions (sarcoplasmic and total protein solubility) in chickens *Pectoralis major* muscles exhibiting macroscopically normal appearance (N) and showing evident signs ascribable to the Wooden Breast (WB) defect.

	Experimental group		P-value
	Normal (N)	Wooden Breast (WB)	
Samples (n.)	62	62	
Water Holding Capacity			
Drip loss (%)	2.53 ± 0.98	2.99 ± 0.96	0.0043
Cooking loss (%)	23.8 ± 5.1	31.0 ± 6.3	<0.0001
Protein solubility (g/100 g of meat)			
Sarcoplasmic proteins	24.9 ± 9.3	23.3 ± 8.1	0.4141
Total proteins	83.2 ± 21.9	81.2 ± 20.5	0.8505

Results and discussion

The findings concerning the effect of WB abnormality on the main quality traits of breast meat are shown in Table 1.

The occurrence of WB defect exerted a remarkable effect on the amount of fluid lost during refrigerated storage and after the application of a heat treatment, as depicted by the significantly higher drip ($P<0.01$) and cooking losses ($P<0.001$) observed in comparison with those measured for N muscles. These findings are in overall agreement with those obtained in previous studies aimed at investigating the impact of WB abnormality on the main quality traits and technological properties of chicken breast meat (Pang et al., 2021; Soglia et al., 2016; Wang et al., 2023). However, the absence of significant differences in proteins' solubility allows us to hypothesize that the impaired WHC observed in WB-affected muscles may not be directly related to differences in the functionality of the proteins themselves. Protein solubility has been widely used as an indirect indicator for protein denaturation (Joo et al., 1999). Therefore, it might be hypothesized that both the sarcoplasmic and the total proteins underwent similar denaturation processes that were not dependent on the onset and progression of the WB defect. A possible role of post-mortem proteolysis (i.e., cytoskeletal protein degradation) in the development of drip loss may be hypothesized (Huff-Lonergan and Lonergan, 2005). In detail, the impaired WHC observed in WB may likely be ascribed to an overall reorganization of the skeletal muscle structure occurring in these PMM that, in its turn, will surely affect the post-mortem water movements across the different muscle compartments and, hence, drip and cooking loss.

As for water properties (Table 2), the occurrence of WB defect is associated with a significant increase in the relative intensity of the proton population ascribable to the water molecules located outside the myofibrillar lattice (32.9 *vs.* 21.5%; $P<0.001$) to the detriment of those trapped in the myofibrillar matrix (62.0 *vs.* 75.4%; $P<0.001$).

In addition, if compared to N, significantly longer transverse relaxation times were observed for the protons ascribable to all the water populations (i.e., bound, intra- and extra-myofibrillar water) in WB. Overall, these findings agree with those obtained in previous studies depicting a substantial re-distribution of the water molecules in WB as a consequence of the microscopic features observed in these PMM (i.e., myodegeneration with occasional regenerative processes, edema, and accumulation of connective tissue) (Choi et al., 2024; Cônsolo et al., 2022; Pang et al., 2020; Soglia et al., 2016). These, in their turn, may also contribute to explain the longer NMR relaxation times observed in WB evidencing a weaker interaction with the different muscular components.

The occurrence of WB abnormality also affects the dielectric properties. Averaged spectra of dielectric constant (ε') and loss factor (ε'') for N and WB samples at 5°C, and related p-level are shown in Fig. 2.

As expected, the dielectric constant and loss factor decrease as a function of frequencies due to the dispersive behavior, which is mainly attributed to the restriction of polarization movements. Similar behavior has been previously observed in poultry meat (Traffano-Schiffo et al., 2017, 2021). A significative difference between averaged N and WB spectra (all p-level ≤ 0.05) can be observed and likely ascribed to the higher water content and availability in WB compared to the N ones. If compared to N, a higher moisture content in WB has been observed in different studies (Dalle Zotte et al., 2017; Soglia et al., 2016; Zhang et al., 2020). Based on the evidence available in the literature, the increased moisture content in WB may likely be attributed to different phenomena taking place within these muscles, including i) an increased deposition of complex carbohydrates (such as glycosaminoglycans) in the extracellular matrix (Velleman and Clark, 2015) and the occurrence of inflammatory processes recalling water by proximal tissues (Petracci et al., 2019; Sihvo et al., 2014; Soglia et al., 2021). The dependence of dielectric properties on water content is widely recognized (Bogale Teseme and Weldemichael Weldeselassie, 2020; Nelson, 2010, 2015; Venkatesh and Raghavan, 2005). As previously reported, a more significant amount of free water contributes to dielectric properties behavior strongly due to the vast availability for polarization movements (Wang et al., 2003, 2008). On the contrary, water interacting with solid structures involve a decrease of real permittivity, due to hydrogen bonds restricting movement (Ryynänen, 1995).

To better understand water solid behavior in chicken breast, dielectric spectra were exploited to calculate relaxation dielectric constant, frequency, and time using Eqs. (2)–(5). Fig. 3 plots the dielectric constant versus the angular velocity (rad/s) to elucidate the dispersive behavior of chicken breasts in the investigated frequency range.

The dielectric constant ($\text{Log}_{10}\ \varepsilon'$) shows two different zones both in N and WB samples, one imputable to β or δ dispersions and one, appearing right after, imputable to γ-relaxation.

Unfortunately, the β or δ dispersion are not entirely visible; thus, the relaxation parameters cannot be calculated. Conversely, the γ-relaxation dielectric constant, frequency, and time are reported in Table 3.

The dielectric constant (ε') of γ relaxation of WB samples (62.0) was significantly higher than the one of N samples (59.8). This means that the WB samples could be polarized more effectively. This was also confirmed by the loss factor (ε'') of γ relaxation of WB samples (19.7), that was significantly higher than the one of N samples (18.3). With an apparent opposite trend, the γ relaxation frequency of WB was at frequencies (1.5 E+09) lower than that of N samples (1.7 E+09). Considering that the relaxation time is directly derived from the WB γ relaxation time, this means that τ_{WB} (1.1E-10) was higher than τ_N (9.6E-11). Since the relaxation event is due to the mobility of molecules, water interacting with solids has a lower relaxation frequency than free water. Debye found the relaxation frequency of pure free liquid water to be around 22 GHz (20°C), and the relaxation of solid water is in the KHz region (Debye, 1934). However, the dielectric properties do not depend only on water but are also significantly influenced by solid macromolecules (Tsoubeli et al., 1995). In addition, the electrical behavior of water depends on the type of particle water interacts with (Batyuk and Kizilova, 2018). As an example, a biopolymers' structure has an influence on dielectric response different from a lipidic structure (Bergo et al., 2012; Iaccheri et al., 2015, 2019, 2023; Kaatze, 1997; Schmidt, 2004; Schwan and Foster, 1977). These premises corroborate the hypothesis of a higher free water content in WB, confirmed by higher values of ε', where the existence of a more complex solid structure can be hypothesized, as underlined by the lower relaxation frequency and the related higher relaxation time. Water in the WB samples could be quantitatively higher but not completely free, because mechanically entrapped by big molecules such as biopolymers. This means that water is not strictly bound to the matrix, because this would lead to a decrease of ε', neither totally free, because this would lead to a relaxation frequency higher in the WB samples than in the N samples. In agreement with this hypothesis, a previous study observed a denser matrix structure in WB (Sanden et al., 2021).

This outcome, together with the not significant difference in

Table 2
Means ± standard deviations of relative intensity (%) and the T_2 (ms) of the proton populations ascribable to the bound, intra- and extra-myofibrillar water in chickens *Pectoralis major* muscles exhibiting macroscopically normal appearance (N) and showing evident signs ascribable to the Wooden Breast (WB) defect.

	N	WB	P-value
Relative intensity (%)			
Bound water	3.2 ± 0.5	2.9 ± 1.1	0.0667
Intra-myofibrillar water	75.4 ± 7.7	62.0 ± 25.2	<0.0001
Extra-myofibrillar water	21.5 ± 8.1	32.9 ± 13.3	<0.0001
T_2 transverse relaxation time (ms)			
Bound water	2.7 ± 1.6	4.4 ± 2.6	<0.0001
Intra-myofibrillar water	41.9 ± 3.0	44.3 ± 6.3	<0.0001
Extra-myofibrillar water	136.4 ± 18.9	150.8 ± 26.4	<0.0001

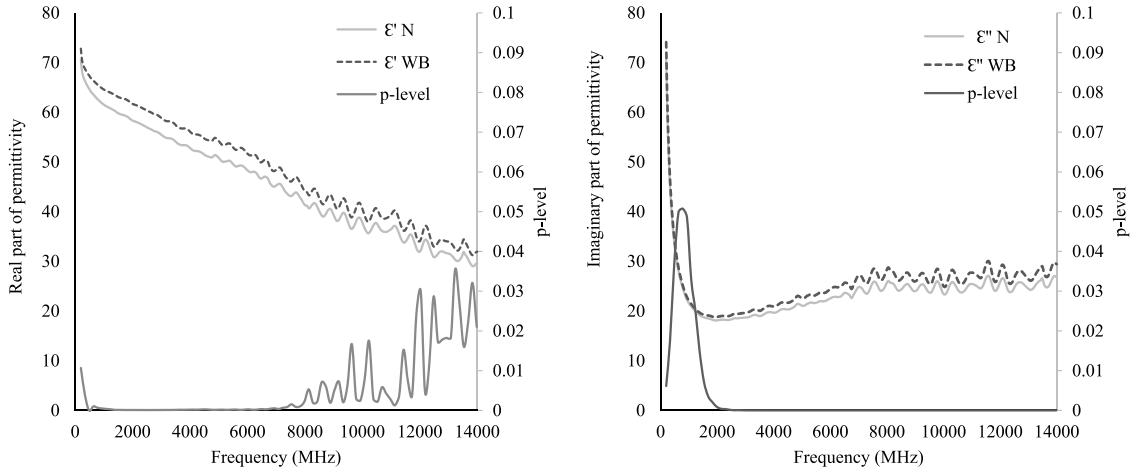

Fig. 2. Mean spectra of dielectric constant (ε') and loss factor (ε'') for breasts macroscopically classified as normal (N, grey continuous line) or wooden breast (WB, dark grey dashed line), and related p-level (p-level $\leq$ 0.05).

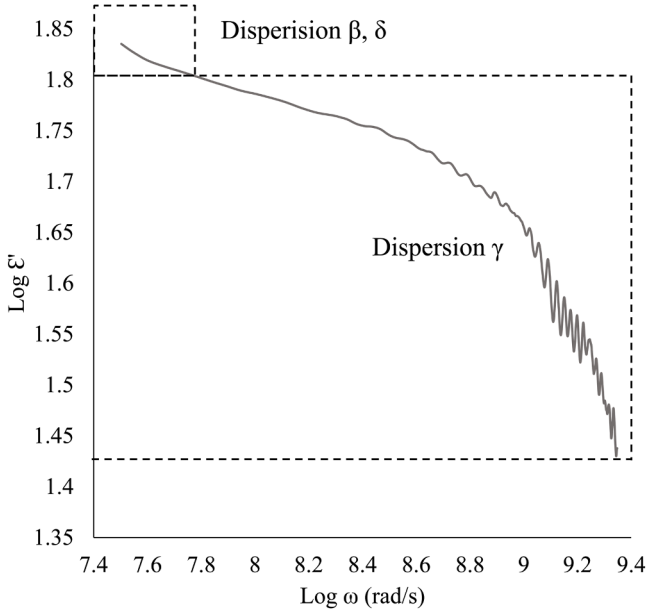

Fig. 3. Dielectric constant (Log_{10} ε') versus angular velocity (Log_{10} rad/s) shows dispersions (as example purpose only one spectra of N sample was shown).

Table 3
Means ± standard deviations of the γ -relaxation dielectric constant (ε'), loss factor (ε''), frequency (GHz) and time (ps) in chickens *Pectoralis major* muscles exhibiting macroscopically normal appearance (N) and showing evident signs ascribable to the Wooden Breast (WB) defect.

	N	WB	P-value
γ-relaxation			
Dielectric constant	59.8 ± 2.1	62.0 ± 3.8	<0.0001
Loss factor	18.3 ± 1.8	19.7 ± 2.1	0.0003
Frequency (GHz)	1.7 ± 0.3	1.5 ± 0.3	0.0003
Time (ps)	96 ± 15	110 ± 31	0.0009

sarcoplasmic and total proteins between N and WB samples described above, allow the attribution of higher WHC in WB samples to the reorganization of skeletal muscle's structure. This also confirms a relevant contribution of the solid structure in the water's behavior, that can be inferred from the relative intensities of the proton populations and from the transverse relaxation times assessed by TD-NMR.

To investigate the relation between DS and NMR, a simple linear regression model relating the loss factor of γ relaxation and NMR raw signal from the samples collected on the first two days was proposed (N= 33, WB=32) (Fig. 4).

The loss factor is a measure of the conversion of kinetic energy into heat, so it was selected to be related to the NMR raw data as an index of biological matrix movement. It can be observed that a poor relationship, even if the estimation is significant (p-level = 6.63 E-06), can be obtained between the data belonging from the two techniques. It can be observed that a decrease in the loss factor corresponds to an NMR signal increase. The amount of water means higher or lower polarization under the DS analysis and could influence NMR measurement, both evidence of modification of physical properties. Further investigations are needed to establish a possible relation between the two techniques, that can be performed on T_2 transverse relaxation time and relaxation time of the different dielectric dispersion, both measures of water-solid dynamics. At the time, a poor direct relation between the two techniques was verified, according to previous work (Kruk et al., 2020), in which only complementary results of DS and TD-NMR on the theoretical relaxation

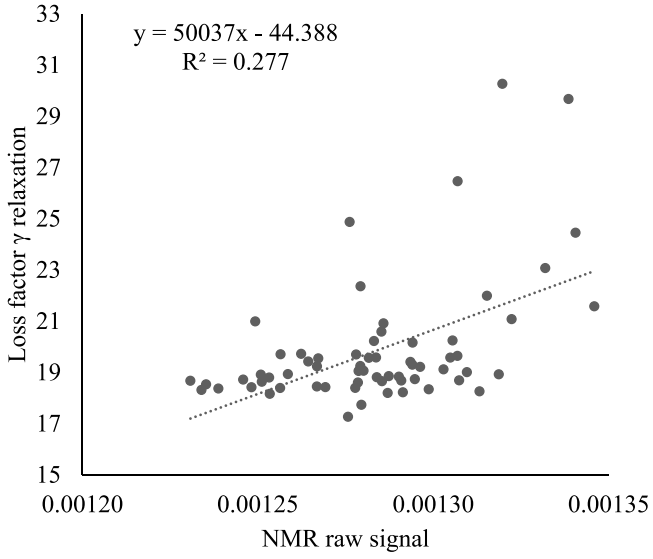

Fig. 4. Loss factor versus NMR signal including chickens *Pectoralis major* muscles exhibiting macroscopically normal appearance and showing evident signs ascribable to the Wooden Breast defect.

processes based on the molecular dynamics and spin interaction links were established.

Conclusions

Chicken breasts affected by WB myopathy were compared to unaffected counterparts using DS and TD-NMR to investigate the interactions between water and solids. Water holding capacity and protein solubility suggest that WB abnormality confers a complex solid structure to breasts muscles, likely imputable to an overall reorganization of the skeletal muscle's structure that, post-mortem, can affect the movements of water across the different muscle compartments, thus justifying the differences in drip and cooking losses. In agreement with this picture, WB led to a significant increase in the relative intensity of the proton population due to the water molecules located outside the myofibrillar lattice and trapped in the myofibrillar matrix.

Dielectric properties further confirm the so hypothesized interactions between solid structure and water. The γ relaxation dielectric constant, loss factor, frequency, and time were significantly different between N and WB samples, showing that chicken breast affected by WB abnormality was characterized by higher free water, inducing higher relaxation dielectric constant and thus polarizability and lower frequency of relaxation imputable to a more complex solid structure.

Future observation could focus on the possibility to further investigate the physical modification of the structures by registering spectra in a wide range of frequencies, to calculate α, β, or δ relaxation. In parallel, the present results could serve as a base for future development of an online DS based technique designed to automatically classify N and WB chicken breasts.

Declaration of competing interest

The authors declare that they have no known competing financial interests or personal relationships that could have appeared to influence the work reported in this paper.

Acknowledgments

The research has been funded by a PRIN National Grant 2022 (Ministry of Education, University and Research) entitled "Shedding new light on the Possible mechanisms underlying broiler CHickens abnormalities: Gallus gallus as animal model for colLagen type 4-related muscle disorders" (Prot. 2022EPWEPW).

Supplementary materials

Supplementary material associated with this article can be found, in the online version, at doi:10.1016/j.psj.2024.104595.

References

Asami, K., 2002. Characterization of biological cells by dielectric spectroscopy. J. Non Cryst. Solids 305, 268–277. https://doi.org/10.1016/S0022-3093(02)01110-9.

Barbut, S., Mitchell, R., Hall, P., Bacon, C., Bailey, R., Owens, C.M., Petracci, M., 2024. Review - myopathies in broilers: supply chain approach to provide solutions to challenges related to raising fast growing birds. Poult. Sci. 103, 103801. https://doi.org/10.1016/j.psj.2024.103801.

Batyuk, L., Kizilova, N., 2018. Modeling of dielectric permittivity of the erythrocytes membrane AS a three-layer model. Development Trends in Medical Science and Practice: the Experience of Countries of Eastern Europe and Prospects of Ukraine. Publishing House "Baltija Publishing. https://doi.org/10.30525/978-9934-571-31-2_2.

Bergo, P., Moraes, I.C.F., Sobral, P.J.A, 2012. Effects of different moisture contents on physical properties of PVA-gelatin films. Food Biophys. 7, 354–361. https://doi.org/10.1007/s11483-012-9273-0.

Bogale Teseme, W., Weldemichael Weldeselassie, H., 2020. Review on the study of dielectric properties of food materials. Am. J. Eng. Technol. Manag. 5, 76. https://doi.org/10.11648/j.ajetm.20200505.11.

Bradford, M.M., 1976. A rapid and sensitive method for the quantitation of microgram quantities of protein utilizing the principle of protein-dye binding. Anal. Biochem. 72, 248–254. https://doi.org/10.1016/0003-2697(76)90527-3.

Choi, J., Shakeri, M., Kim, W.K., Kong, B., Bowker, B., Zhuang, H., 2024. Water properties in intact wooden breast fillets during refrigerated storage. Poult. Sci. 103, 103464. https://doi.org/10.1016/j.psj.2024.103464.

Cole, K.S., Cole, R.H., 1941. Dispersion and absorption in dielectrics I. Alternating current characteristics. J. Chem. Phys. 9, 341–351. https://doi.org/10.1063/1.1750906.

Cônsolo, N.R.B., Barbosa, L.C.G.S., Moraes, T.B., Buraque, V.M., Colnago, L.A., Queiroz Júnior, L.H.K., Oliveira, V.M., Hannaford, R., Araújo, C.S.S., Roque, F., de, A., Granghelli, C.A., Fonseca, A.C., Araújo, L.F., 2022. Using TD-NMR relaxometry to assess the effects of diet type and stocking rate on the incidence and degree of severity of myopathies in broilers. Microchem. J. 181, 107745. https://doi.org/10.1016/j.microc.2022.107745.

Dalgaard, L.B., Rasmussen, M.K., Bertram, H.C., Jensen, J.A., Møller, H.S., Aaslyng, M.D., Hejbøl, E.K., Pedersen, J.R., Elsser-Gravesen, D., Young, J.F., 2018. Classification of wooden breast myopathy in chicken pectoralis major by a standardised method and association with conventional quality assessments. Int. J. Food Sci. Technol. 53, 1744–1752. https://doi.org/10.1111/ijfs.13759.

Dalle Zotte, A., Tasoniero, G., Puolanne, E., Remignon, H., Cecchinato, M., Catelli, E., Cullere, M., 2017. Effect of "wooden breast" appearance on poultry meat quality, histological traits, and lesions characterization. Czech J. Anim. Sci. 62, 51–57. https://doi.org/10.17221/54/2016-CJAS.

Debye, P., 1934. Part I. Dielectric constant. Energy absorption I N dielectrics with polar molecules. Trans. Faraday Soc. 30, 679–684.

Fukuzaki, M., Miura, N., Shinyashiki, N., Kurita, D., Shioya, S., Haida, M., Mashimo, S., 1995. Comparison of water relaxation time in serum albumin solution using nuclear magnetic resonance and time domain reflectometry. J. Phys. Chem 99, 431–435. https://doi.org/10.1021/j100001a064.

Gabriel, S., Lau, R.W., Gabriel, C., 1996. The dielectric properties of biological tissues: III. Parametric models for the dielectric spectrum of tissues. Phys. Med. Biol. 41, 2271–2293. https://doi.org/10.1088/0031-9155/41/11/003.

Havriliak, S., Negami, S., 1967. A complex plane representation of dielectric and mechanical relaxation processes in some polymers. Polymer 8, 161–210. https://doi.org/10.1016/0032-3861(67)90021-3.

Huff-Lonergan, E., Lonergan, S.M., 2005. Mechanisms of water-holding capacity of meat: the role of postmortem biochemical and structural changes. Meat. Sci. 71, 194–204. https://doi.org/10.1016/j.meatsci.2005.04.022.

Hurt, W.D., 1985. Corm unications multiterm debye dispersion relations for permittivity of muscle. IEEE Trans. Biomed. Eng. 32, 60–64. https://doi.org/10.1109/TBME.1985.325629.

Iaccheri, E., Laghi, L., Cevoli, C., Berardinelli, A., Ragni, L., Romani, S., Rocculi, P., 2015. Different analytical approaches for the study of water features in green and roasted coffee beans. J. Food Eng. 146, 28–35. https://doi.org/10.1016/j.jfoodeng.2014.08.016.

Iaccheri, E., Ragni, L., Cevoli, C., Romani, S., Dalla Rosa, M., Rocculi, P., 2019. Glass transition of green and roasted coffee investigated by calorimetric and dielectric techniques. Food Chem. 301, 125187. https://doi.org/10.1016/j.foodchem.2019.125187.

Iaccheri, E., Siracusa, V., Ragni, L., De Aguiar Saldanha Pinheiro, A.C., Romani, S., Rocculi, P., Dalla Rosa, M., Sobral, P.J., do, A., 2023. Studying physical state of films based on casava starch and/or chitosan by dielectric and thermal properties and effects of pitanga leaf hydroethanolic extract. J. Food Eng. 339, 111280. https://doi.org/10.1016/j.jfoodeng.2022.111280.

Joo, S.T., Kauzman, R.G., Kim, B.C., Park, G.B., 1999. The relationship of sarcoplasmic and myobrillar protein solubility to colour and water-holding capacity in porcine longissimus muscle. Meat. Sci. 52, 291–297. https://doi.org/10.1016/s0309-1740(99)00005-4.

Kaatze, U., 1997. The dielectric properties of water in its different states of interaction. J. Solut. Chem. 26, 1049–1112. https://doi.org/10.1007/BF02768829.

Kent, M., Anderson, D., 1996. Dielectric studies of added water in poultry meat and scallops. J. Food Eng. 28, 239–259. https://doi.org/10.1016/0260-8774(95)00064-X.

Kruk, D., Masiewicz, E., Wojciechowski, M., Florek-Wojciechowska, M., Broche, L.M., Lurie, D.J., 2020. Slow dynamics of solid proteins – Nuclear magnetic resonance relaxometry versus dielectric spectroscopy. J. Magn. Reson. 314, 106721. https://doi.org/10.1016/j.jmr.2020.106721.

Kuang, W., Nelson, S.O., 1998. Low-frequency dielectric properties of biological tissues: a review with some new insights. Trans. Am. Soc. Agric. Eng. 41, 173–184. https://doi.org/10.13031/2013.17142.

Lawrence, J.H., Tobias, C.A., Curtis, H.J., Gray, L.H., Thorell, B.O., 1957. In: Lawrence, J. H., Cornelius, T.A. (Eds.), Advances in Biological and Medical Physics, V. Academic Press INC.

Markx, G.H., Davey, C.L., 1999. The dielectric properties of biological cells at radiofrequencies: applications in biotechnology. Enzyme Microb. Technol. 25, 161–171. https://doi.org/10.1016/S0141-0229(99)00008-3.

Morey, A., Smith, A.E., Garner, L.J., Cox, M.K., 2020. Application of bioelectrical impedance analysis to detect broiler breast filets affected with Woody breast myopathy. Front. Physiol. 11, 808. https://doi.org/10.3389/fphys.2020.00808.

Mudalal, S., Babini, E., Cavani, C., Petracci, M., 2014. Quantity and functionality of protein fractions in chicken breast fillets affected by white striping. Poult. Sci. 93, 2108–2116. https://doi.org/10.3382/ps.2014-03911.

Nelson, S.O., 2010. Fundamentals of dielectric properties measurements and agricultural applications. J. Microw. Power Electromagn. Energy 44, 98–113. https://doi.org/10.1080/08327823.2010.11689778.

Nelson, S.O., 2015. Dielectric properties of agricultural materials and their applications. Academic Press. https://doi.org/10.1016/C2014-0-02694-9.
Nelson, S.O., Trabelsi, S., Zhuang, H., 2007. Dielectric spectroscopy of fresh chicken breast meat. In: Proceedings of the 2007 ASABE Annual International Meeting. doi: 10.13031/2013.23194.
O'Toole, M.D., Glowacz, M., Peyton, A.J., 2023. Bioimpedance measurement of avocado fruit using magnetic induction spectroscopy. IEEE Trans. AgriFood Electron. 1, 99–107. https://doi.org/10.1109/tafe.2023.3303177.
Pang, B., Bowker, B., Zhang, J., Yang, Y., Zhuang, H., 2020. Prediction of water holding capacity in intact broiler breast fillets affected by the woody breast condition using time-domain NMR. Food Control 118, 107391. https://doi.org/10.1016/j.foodcont.2020.107391.
Pang, B., Yu, X., Bowker, B., Zhang, J., Yang, Y., Zhuang, H., 2021. Effect of meat temperature on moisture loss, water properties, and protein profiles of broiler pectoralis major with the woody breast condition. Poult. Sci. 100, 1283–1290. https://doi.org/10.1016/j.psj.2020.10.034.
Petracci, M., Laghi, L., Rocculi, P., Rimini, S., Panarese, V., Cremonini, M.A., Cavani, C., 2012. The use of sodium bicarbonate for marination of broiler breast meat. Poult. Sci. 91, 526–534. https://doi.org/10.3382/ps.2011-01753.
Petracci, M., Soglia, F., Madruga, M., Carvalho, L., Ida, E., Estévez, M., 2019. Wooden-breast, white striping, and spaghetti meat: causes, consequences and consumer perception of emerging broiler meat abnormalities. Comprehensive Reviews in Food Science and Food Safety 18, 565–583. https://doi.org/10.1111/1541-4337.12431.
Ryynänen, S., 1995. The electromagnetic properties of food materials: a review of the basic principles. J. Food Eng. 26, 409–429. https://doi.org/10.1016/0260-8774(94)00063-F.
Sanden, K.W., Böcker, U., Ofstad, R., Pedersen, M.E., Høst, V., Afseth, N.K., Rønning, S. B., Pleshko, N., 2021. Characterization of collagen structure in normal, wooden breast and spaghetti meat chicken fillets by ftir microspectroscopy and histology. Foods 10, 548. https://doi.org/10.3390/foods10030548.
Schmidt, S.J., 2004. Water and solids mobility in foods. Adv. Food Nutr. Res. 48, 1–101. https://doi.org/10.1016/S1043-4526(04)48001-2.
Schwan, H.P., Foster, K.R., 1977. Microwave dielectric properties of tissue. Some comments on the rotational mobility of tissue water. Biophys. J. 17, 193–197. https://doi.org/10.1016/S0006-3495(77)85637-3.
Sihvo, H.K., Immonen, K., Puolanne, E., 2014. Myodegeneration with fibrosis and regeneration in the pectoralis major muscle of broilers. Vet. Pathol. 51, 619–623. https://doi.org/10.1177/0300985813497488.
Soglia, F., Laghi, L., Canonico, L., Cavani, C., Petracci, M., 2016. Functional property issues in broiler breast meat related to emerging muscle abnormalities. Food Res. Int. 89, 1071–1076. https://doi.org/10.1016/j.foodres.2016.04.042.
Soglia, F., Petracci, M., Davoli, R., Zappaterra, M., 2021. A critical review of the mechanisms involved in the occurrence of growth-related abnormalities affecting broiler chicken breast muscles. Poult. Sci. 100, 101180. https://doi.org/10.1016/j.psj.2021.101180.
Tanaka, F., Mallikarjunan, P., Kim, C., Hung, Y.C., 2000. Measurement of dielectric properties of chicken breast meat. J. Japanese Soc. Agric. Mach. 62, 109–119. https://doi.org/10.11357/jsam1937.62.4_109.
Traffano-Schiffo, M.V., Castro-Giraldez, M., Colom, R.J., Fito, P.J., 2017. Development of a spectrophotometric system to detect white striping physiopathy in whole chicken carcasses. Sensors 17, 1024. https://doi.org/10.3390/s17051024.
Traffano-Schiffo, M.V., Chuquizuta, T., Castro-Giraldez, M., Fito, P.J., 2021. Development of a methodology to categorize poultry meat affected by deep pectoral myopathy. J. Food Process. Preserv. 45, e15226. https://doi.org/10.1111/jfpp.15226.
Tran, V.N., Stuchly, S.S., 1987. Dielectric properties of beef, beef liver, chicken and salmon at frequencies from 100 TO 2500 MHz. J. Microw. Power Electromagn. Energy 22, 29–33. https://doi.org/10.1080/08327823.1987.11688003.
Tsoubeli, M.N., Davis, E.A., Gordon, J., 1995. Dielectric properties and water mobility for heated mixturesof starch, milk protein, and water. Cereal. Chem. 72, 64–69.
Velleman, S.G., Clark, D.L., 2015. Histopathologic and myogenic gene expression changes associated with wooden breast in broiler breast muscles. Avian Dis. 59, 410–418. https://doi.org/10.1637/11097-042015-Reg.1.
Venkatesh, M.S., Raghavan, G.S.V., 2005. An overview of dielectric properties measuring techniques. Can. Biosyst. Eng. 47, 15–30.
Wang, C., Che, S., Susta, L., Barbut, S., 2023. Textural and physical properties of breast fillets with myopathies (wooden breast, white striping, spaghetti meat) in Canadian fast-growing broiler chickens. Poult. Sci. 102, 102309. https://doi.org/10.1016/j.psj.2022.102309.
Wang, Y., Tang, J., Rasco, B., Kong, F., Wang, S., 2008. Dielectric properties of salmon fillets as a function of temperature and composition. J. Food Eng. 87, 236–246. https://doi.org/10.1016/j.jfoodeng.2007.11.034.
Wang, Y., Wig, T.D., Tang, J., Hallberg, L.M., 2003. Dielectric properties of foods relevant to RF and microwave pasteurization and sterilization. J. Food Eng. 57, 257–268. https://doi.org/10.1016/S0260-8774(02)00306-0.
Warner, R.D., Kauffman, R.G., Greaser, M.L., 1997. Muscle protein changes post mortem quality traits relation to pork quality traits. Meat. Sci. 45, 339–352. https://doi.org/10.1016/s0309-1740(96)00116-7.
Wolf, M., Gulich, R., Lunkenheimer, P., Loidl, A., 2012. Relaxation dynamics of a protein solution investigated by dielectric spectroscopy. Biochim. Biophys. Acta Proteins Proteom. 1824, 723–730. https://doi.org/10.1016/j.bbapap.2012.02.008.
Zhang, Y., Wang, P., Xu, X., Xia, T., Li, Z., Zhao, T., 2020. Effect of wooden breast myopathy on water-holding capacity and rheological and gelling properties of chicken broiler breast batters. Poult. Sci. 99, 3742–3751. https://doi.org/10.1016/j.psj.2020.03.032.